

RECEIVED

OCT 12 1999

Results from Experiment E917 for Au + Au Collisions at the **OSTI**D. J. Hofman^a

for the E917 collaboration*

B.B. Back^a, R.R. Betts^{a,c}, J. Chang^b, W.C. Chang^b, C.Y. Chi^d, Y.Y. Chu^e,
 J.B. Cumming^e, J.C. Dunlop^f, W. Eldredge^b, S.Y. Fung^b, R. Ganz^{c,g}, E. Garcia^h,
 A. Gillitzer^{a,i}, G. Heintzelman^{f,e}, W.F. Henning^a, D.J. Hofman^a, B. Holzman^c,
 J.H. Kang^j, E.J. Kim^j, S.Y. Kim^j, Y. Kwon^j, D. McLeod^c, A.C. Mignerey^h,
 M. Moulson^k, V. Nanal^{a,l}, C.A. Ogilvie^f, R. Pak^m, A. Ruangma^h, D. Russ^h, R. Seto^b,
 P.J. Stankas^h, G.S.F. Stephans^f, H. Wang^b, F.L.H. Wolfs^m, A.H. Wuosmaa^a,
 H. Xiang^b, G.H. Xu^b, H. Yao^f, C.M. Zou^b

^aArgonne National Laboratory, Argonne, IL, USA 60439^bUniversity of California Riverside, Riverside, CA, USA 92521^cUniversity of Illinois at Chicago, Chicago, IL, USA 60607^dColumbia University, Nevis Laboratories, Irvington, NY, USA 10533^eBrookhaven National Laboratory, Chemistry Department, Upton, NY, USA 11973^fMassachusetts Institute of Technology, Cambridge, MA, USA 02139^gMax Planck Institut für Physik, D-80805 München, Germany^hUniversity of Maryland, College Park, MD, USA 20742ⁱTechnische Universität München, D-85748 Garching, Germany^jYonsei University, Seoul 120-749, South Korea^kLaboratori Nazionali di Frascati, INFN, 00044 Frascati, Italy^lTata Institute of Fundamental Research, Colaba, Mumbai 400005, India^mUniversity of Rochester, Rochester, NY, USA 14627

The effects of baryon stopping and its resulting energy deposition on the dynamics of Au + Au collisions at 6, 8 and 10.8 GeV/nucleon are explored with recent results from the AGS experiment E917. Current analyses of stopping, collective flow signals and HBT parameters are presented. Strangeness and anti-baryon production is examined using the yields of anti-lambdas and anti-protons.

1. INTRODUCTION

Although much has been learned about relativistic heavy ion collisions in the past decade, a complete understanding of some of the most basic questions has yet to be fully

*This work was supported by the U.S. Department of Energy, the National Science Foundation (USA) and KOSEF (Korea).

DISCLAIMER

This report was prepared as an account of work sponsored by an agency of the United States Government. Neither the United States Government nor any agency thereof, nor any of their employees, make any warranty, express or implied, or assumes any legal liability or responsibility for the accuracy, completeness, or usefulness of any information, apparatus, product, or process disclosed, or represents that its use would not infringe privately owned rights. Reference herein to any specific commercial product, process, or service by trade name, trademark, manufacturer, or otherwise does not necessarily constitute or imply its endorsement, recommendation, or favoring by the United States Government or any agency thereof. The views and opinions of authors expressed herein do not necessarily state or reflect those of the United States Government or any agency thereof.

DISCLAIMER

Portions of this document may be illegible in electronic image products. Images are produced from the best available original document.

realized. The character and amount of stopping achieved in these collisions as reflected in the spectral shapes and rapidity distributions of protons are still not completely understood. The degree of collectivity and the effects of pressure gradients in the hot collision zone manifested in the azimuthal distributions of both protons and produced particles is of current interest. At AGS energies, information gained by the study of produced particles which contain strange quarks has also been dramatically expanded through measurements of K, ϕ -meson and Λ production.

One of the goals of experiment E917 has been to more fully characterize these collisions by studying their properties as a function of bombarding energy. To further this goal, particle spectra were measured at beam energies of 6, 8 and 10.8 GeV/nucleon. This systematic approach is critical in the ongoing search for new phenomena, the signatures of which may only become visible when viewed over a wide energy scale. A second objective of the experiment, to focus on ϕ -meson, $\bar{\Lambda}$ and \bar{p} production, was attained by devoting most of the beam time to running at the highest energy, 10.8 GeV/nucleon, utilizing a two-Kaon and anti-proton trigger.

2. EXPERIMENT

Experiment E917 utilized the same 0.4-Tesla Henry Higgins magnetic spectrometer as the prior experiment E866. This spectrometer combines an angular acceptance of 25msr with excellent particle identification and momentum resolution. Particle identification is provided by a combination of drift chambers on either side of the magnet and a 130ps resolution time-of-flight wall. The momentum resolution is $\Delta p/p \leq 2\%$. More details of the spectrometer and associated data analysis can be found in References [1,2].

Three modifications to the experimental setup were specific to experiment E917. First, the data acquisition system was upgraded to handle 2.5 times higher data rates. Second, the acceptance was increased with the installation of a larger tracking chamber in front of the magnet. Finally, a beam vertexing detector system was developed and installed to provide a precise determination of the trajectory ($\sigma \simeq 150\mu\text{m}$ at the target) of each incident Au beam particle [3].

3. PARTICLE YIELDS

A complete study of particle emission as a function of bombarding energy and centrality provides a first step towards understanding the dynamics of these collisions. The invariant yields of protons were determined at 6, 8 and 10.8 GeV/nucleon by fitting the spectra as a function of transverse mass, m_t , using a Boltzmann distribution. These fits were used to derive the total probability for proton emission per unit of rapidity, dN/dy , and inverse slopes, T , at each energy with a series of centrality gates. The results for the most central 5% of collisions are shown in Fig. 1 for all three bombarding energies.

The main characteristics of the proton yields (see Fig. 1) are a wide distribution in dN/dy and values of the inverse slope, T , which peak at mid-rapidity. The solid curves represent the results expected for isotropic emission from a thermal source at rest in the center-of-mass system with an "effective" temperature, T_0 . For this simple source, the rapidity dependence of the inverse slope is given by $T = T_0/\cosh y$ and the distribution in dN/dy is derived from T assuming a Boltzmann distribution for the m_t yields [4].

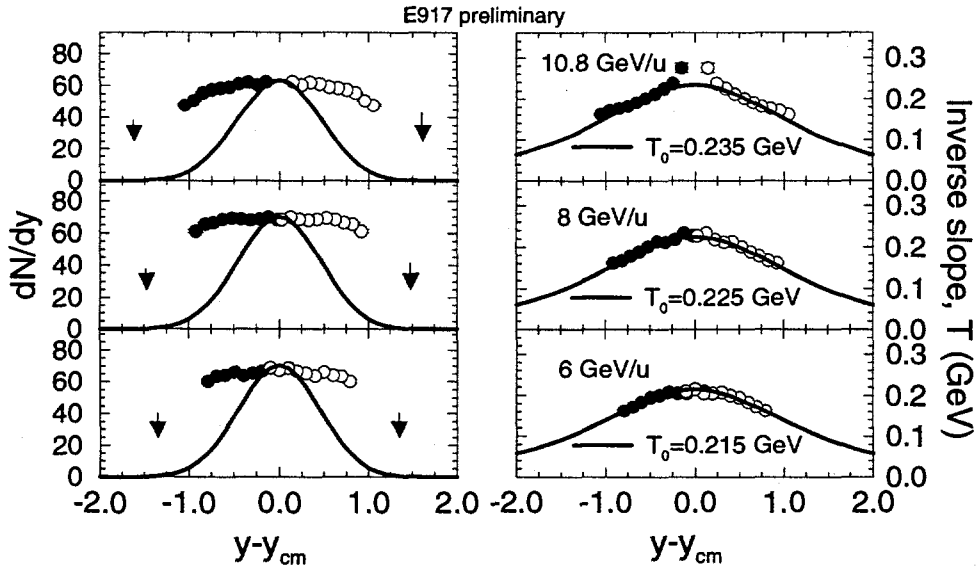


Figure 1. Proton rapidity distributions for the central 5% of collisions in the center-of-mass system (left panels) and inverse slopes from the Boltzmann fits (right panels) are compared to a simple thermal source prediction for the three beam energies. Arrows indicate target and beam rapidities. Solid points are the measured data and open circles are the same data points reflected about mid-rapidity by symmetry.

In the preliminary analysis of the proton spectra we find that the inverse slope values are in reasonable agreement with the $1/\cosh y$ dependence (right side of Fig. 1). This agreement is likely fortuitous, however, as the corresponding predicted distributions in dN/dy are too narrow to describe the experimental data (left side of Fig. 1). A superposition of sources at different rapidity with the same T_0 is able to describe the measured distribution in dN/dy , but the resulting m_t spectra fail to reproduce the experimental inverse slope rapidity dependence. A simultaneous description of dN/dy and $T_{exp}(y)$ can be obtained by allowing for a rapidity dependent T_0 parameter. The observed width of the proton yield in dN/dy may, therefore, directly indicate a significant degree of longitudinal expansion, incomplete stopping, or perhaps some combination of both effects.

The question of stopping and expansion can be more fully addressed by also studying produced particles. Experiment E917 contributes to this effort by measuring kaon, ϕ -meson, anti-lambda and anti-proton yields. The kaon and ϕ -meson results will be discussed elsewhere in these proceedings [5,6], and anti-baryons will be discussed in Section 6.

4. FLOW

The study of collective flow in relativistic nucleus-nucleus collisions provides unique insight into the complicated dynamics of these reactions. These flow observables may carry information about such processes as thermalization, mean-field effects, phase transitions or even the possible creation of the quark-gluon plasma. A possible plasma phase may cause the pressure gradient from the baryon dense region to be reduced, or even entirely absent. In addition, flow signals for produced particles (e.g. pions, kaons, anti-protons) may yield

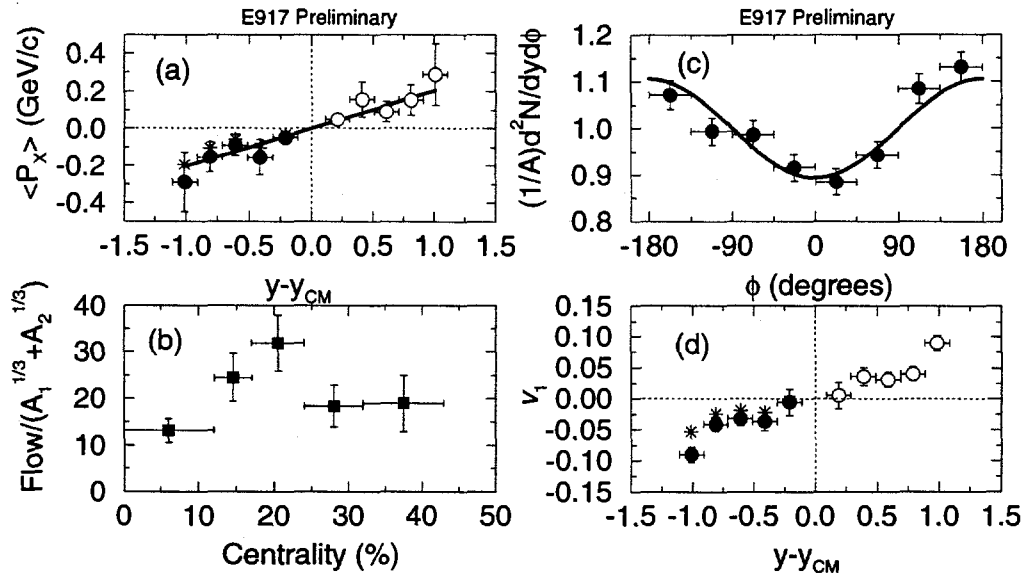


Figure 2. Preliminary directed flow results for protons in Experiment E917. Panel (a) shows $\langle P_x \rangle$ for centrality 17-24% and panel (b) gives the flow magnitude as a function of centrality. Panel (c) contains the azimuthal distribution of $d^2N/dy d\phi$ for centrality 17-24% and rapidity $y = 0.6$ fit with the first term, v_1 , in the Fourier series. Panel (d) displays the extracted v_1 coefficients as a function of rapidity. In panels (a) and (d), stars represent the measured values before correction for the reaction plane resolution and solid points with error bars are after the correction has been applied. Open points are the measured (and corrected) data reflected about mid-rapidity by symmetry.

important information on the magnitude of re-scattering or absorption processes.

Central to any study of flow is the ability to measure the reaction plane on an event-by-event basis. The main experimental components of the flow analysis are a beam vertexing detector [3] located in front of the target, a hodoscope located 11.4 meters downstream from the target to measure the distribution of light (e.g. proton, deuteron) charged particles from the beam remnant, and the movable magnetic spectrometer to measure particle yields relative to the deduced reaction plane.

Preliminary directed flow results at 10.8 GeV/nucleon for the protons, shown in Fig. 2, were extracted utilizing both a calculation of the mean proton momentum along the beam impact parameter, $\langle P_x \rangle$, and the method of Fourier component analysis. In both cases the proton m_t spectra for each centrality, rapidity and reaction plane angle bin are fit to Boltzmann distributions.

Since the data are measured in the target rapidity region, positive directed flow corresponds to an excess yield of particles 180° away from the impact parameter \vec{b} . Thus the deduced $\langle P_x \rangle$ should be negative in the target rapidity region and the $d^2N/dy d\phi$ distribution for $y=0.6$ should exhibit an excess yield at $\phi = \pm 180^\circ$. Both trends are clearly evident in Fig. 2(a,c).

The centrality dependence of the deduced flow magnitude is given in Fig. 2(b), where the flow signal has been derived from the slope of a straight line fit to the $\langle P_x \rangle$ values corrected for reaction plane resolution at mid-rapidity, i.e. $\text{Flow} = y_{cm} \times d\langle P_x \rangle / dy|_{y=y_{cm}}$.

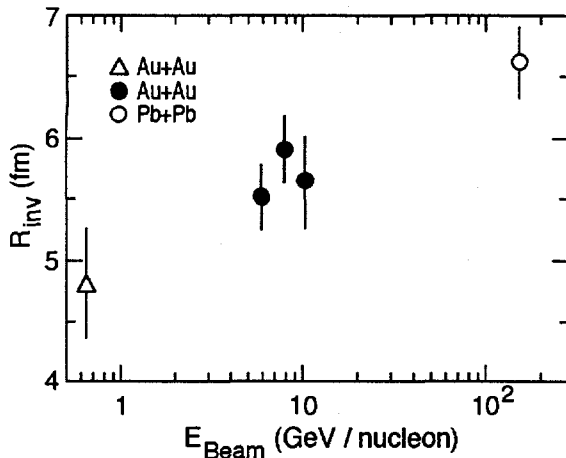


Figure 3. Energy dependence of the one-dimensional source radii obtained from Hanbury-Brown-Twiss analysis of $\pi^-\pi^-$ pairs. The open triangle (Δ) is Plastic Ball data from Ref. [7], the solid circles (\bullet) are the *preliminary* E917 results, and the open circle (\circ) is NA44 data from Ref. [8].

The directed flow signal is a strong function of centrality, increasing to a maximum for mid-central collisions.

The rapidity dependence of the extracted Fourier v_1 coefficients and a mid-central event selection (17-24% centrality) is shown in Fig. 2(d). The first Fourier coefficient was obtained using a fit of the form $d^2N/dy d\phi = A(1 + 2v_1 \cos(\phi))$.

A clear positive directed flow signal for the protons sets a solid baseline for an investigation of the flow of produced particles currently underway.

5. PION INTERFEROMETRY

The space-time extent of the nuclear fireball from which various particle species originate can be estimated by applying the Hanbury-Brown-Twiss (HBT) analysis to pairs of identical particles. As a first step in this analysis, one-dimensional correlation functions were obtained from the data and the invariant radius parameter, R_{inv} , was extracted from the fits for 6, 8 and 10.8 GeV/nucleon.

Preliminary one-dimensional HBT results for $\pi^-\pi^-$ pairs from E917 are compared to similar analysis results obtained at both lower and higher energy in Fig. 3. This simple parameterization gives an estimate of the volume of the emitting system and we find no difference over the 6-10.8 GeV/nucleon bombarding energy range covered by experiment E917. However, we do observe a distinct trend of increasing source size with beam energy across the much larger energy region covered by GSI/SIS [7], E917 and CERN/SPS [8].

6. ANTI-BARYONS

The study of anti-lambda ($\bar{\Lambda}$) and anti-proton (\bar{p}) production is of particular interest because changes in their production could be sensitive to the density and temperature produced in the collision. The $\bar{\Lambda}/\bar{p}$ ratio, in particular, is of interest because it reflects the \bar{s}/\bar{u} quark production ratio which could increase strongly if a quark-gluon plasma is created.

Experiment E917 measured \bar{p} and $\bar{\Lambda}$ particle yields in the rapidity range $1.0 < y < 1.4$. The signal for $\bar{\Lambda}$ particles was reconstructed from $\bar{p}\pi^+$ pairs, and is clearly seen in the invariant mass distribution of Fig. 4(a). The transverse mass spectra of \bar{p} and $\bar{\Lambda}$ particles

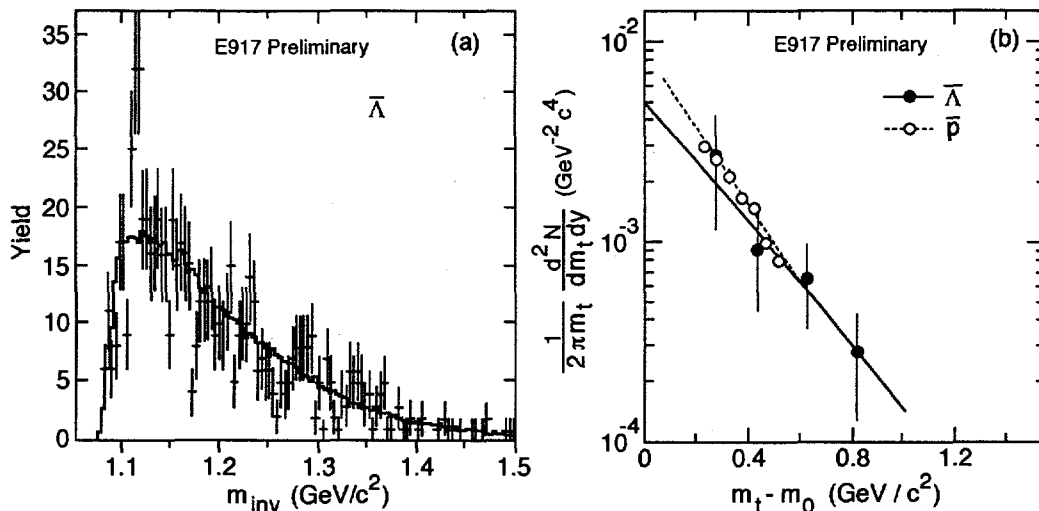


Figure 4. The invariant mass spectrum, m_{inv} , reconstructed from $\bar{p}\pi^+$ pairs is given in panel (a). The solid curve represents the fitted mixed-event background. Panel (b) shows the transverse mass (m_t) spectra of $\bar{\Lambda}$ (\bullet) and \bar{p} (\circ) for 0-23% central events.

for central 0–23% events are displayed in Fig. 4(b).

In order to extract the $\bar{\Lambda}/\bar{p}$ ratio, the yield of anti-protons directly produced in the collision, \bar{p}_{direct} , was obtained by assuming that the decay of $\bar{\Lambda}$ is the only source of hyperon feed-down into the experimentally measured \bar{p} yield. With this assumption, the yield of direct anti-protons can be obtained by correcting for the 64.2% branching ratio of the $\bar{\Lambda}$ decay into the $\bar{p}\pi^+$ channel. The result of this analysis is given in Table 1.

As shown in Table 1, the E917 measure of the $\bar{\Lambda}/\bar{p}$ ratio is greater than unity for the 0-23% central Au + Au collisions. This value is consistent with the E859 measurement for central collisions in the Si+Au system of $\bar{\Lambda}/\bar{p}_{direct} = 2.9 \pm 0.9 \pm 0.5$ [9]. A lower limit on this ratio of $\bar{\Lambda}/\bar{p}_{direct} \geq 2.8$ (98% C.L.) was inferred by experiment E864 [10] for central Au + Pb collisions at 11.5A GeV/c from the difference between the E864 and E878 [11] \bar{p} measurements. This limit also lies within the bounds of the E917 result. It should be noted that several differences do exist between the various measurements of the $\bar{\Lambda}/\bar{p}$ ratio, specifically in the range of transverse mass, rapidity and centrality. Nevertheless, in all cases a $\bar{\Lambda}/\bar{p}$ ratio greater than one has been observed for central events, and this result may point to evidence of new physics phenomena.

7. SUMMARY AND OUTLOOK

An analysis of transverse mass spectra for protons emitted in central Au+Au collisions at beam kinetic energies of 6, 8 and 10.8 GeV/nucleon reveals wide distributions in dN/dy which cannot be described by a simple thermal model assuming isotropic emission from a source at rest in the center-of-mass system. The measured proton distributions in dN/dy can be interpreted as a manifestation of longitudinal expansion and/or incomplete stopping. Strong directed flow signals for the protons were observed and ongoing analysis will examine flow signals for produced particles. The one-dimensional HBT analysis

Table 1

$\bar{\Lambda}$ and \bar{p} results for Au + Au collisions at 10.8 GeV/nucleon in experiment E917. The rapidity range is $1.0 < y < 1.4$, and the error bars are statistical.

Centrality	$\bar{\Lambda} dN/dy$	T	$\bar{p}_{\text{direct}} dN/dy$	$\bar{\Lambda}/\bar{p}_{\text{direct}}$
Minimum Bias	$5.6_{-1.6}^{+2.3} \times 10^{-3}$	227_{-48}^{+84}	$3.7_{-1.5}^{+1.0} \times 10^{-3}$	$1.5_{-0.7}^{+1.9}$
Central 0–23%	$1.56_{-0.45}^{+0.64} \times 10^{-2}$	232_{-51}^{+92}	$0.50_{-0.41}^{+0.29} \times 10^{-2}$	$3.1_{-1.7}^{+2.0}$

All data in this table are *preliminary* E917 results.

of pions gives values of the invariant radii, R_{inv} , which fit smoothly to the systematic dependence of this quantity as a function of bombarding energy. In all these cases, no evidence exists of a departure from expectations based on purely hadronic scenarios.

One of the exciting results from experiment E917 is a measure of the $\bar{\Lambda}/\bar{p}$ ratio which is larger than unity. A ratio larger than one may signify new physics phenomena beyond a purely hadronic model, but further theoretical work will be required to quantify this possibility.

Data analysis for E917 continues to increase the available statistics and expand the analysis possibilities. Future work will include flow results at 8 GeV as well as flow for produced particles. With increased statistics, the HBT analysis will allow for a study of any possible reaction plane dependencies of source sizes as well as multi-dimensional parameter extraction. Proton and $\bar{\Lambda}$ data for non-central events will also become available, opening a relatively unexplored region for detailed comparisons to models.

REFERENCES

1. L. Ahle *et al.*, Phys. Rev. **C57** (1998) 466.
2. T. Abbott *et al.*, Nucl. Instr. and Meth. **A290** (1990) 41.
3. B.B. Back *et al.*, Nucl. Instr. and Meth. **A412** (1998) 191.
4. E. Schnedermann *et al.*, Phys. Rev. **C48** (1993) 2462.
5. J.C. Dunlop (E917 Collaboration), these proceedings.
6. R. Seto (E917 Collaboration), these proceedings.
7. R. Bock *et al.*, Z. Phys. **A333** (1989) 193.
8. I.G. Bearden *et al.*, Phys. Rev. **C58** (1998) 1656.
9. G.S. Stephans and Y. Wu, J. Phys **G23** (1997) 1895.
10. T.A. Armstrong *et al.*, Phys. Rev. Lett. **79** (1997) 3351; Los Alamos preprint nucl-ex/9811002; G.J. Wang *et al.*, Los Alamos preprint nucl-th/9807036 and nucl-th/9806006.
11. D. Beavis *et al.*, Phys Rev. Lett. **75** (1995) 3078; Phys. Rev. **C56** (1997) 1521.